Effects of Optical Feedback on Static and Dynamic Characteristics of Vertical-Cavity Surface-Emitting Lasers

Joanne Y. Law and Govind P. Agrawal, *Fellow, IEEE*

***Abstract*—We present a numerical study of the effects of optical feedback on the static and dynamic characteristics of vertical-cavity surface-emitting lasers (VCSEL's) under both single-mode and two-mode operations. Our model includes transverse effects such as carrier diffusion and spatial hole burning (SHB) and is therefore capable of including gain-saturation-induced coupling among transverse modes. For short external cavities ($\sim$30 μm), optical feedback can completely suppress higher order transverse modes. For relatively long external cavities ($\sim$1 cm), VCSEL's follow a period-doubling route to chaos. Numerical results show that multimode VCSEL's exhibit self-pulsations at higher feedback levels compared with the single-mode case.**

***Index Terms*— Chaos, laser mode, semiconductor lasers, surface-emitting lasers.**

I. Introduction

VERTICAL-CAVITY surface-emitting lasers (VCSEL's) have been studied extensively over the past few years because of their useful characteristics such as a low threshold current, single-longitudinal-mode operation, circular output beam, and wafer-scale integrability [1], [2]. Because of these advantages, VCSEL's are attractive as compact light sources for applications in optical communications and interconnects. In such applications, when light from a VCSEL is focused onto an optical fiber or an optical disc, some light is invariably reflected back into the laser. Experimental investigations demonstrate that VCSEL performance is strongly affected by the presence of optical feedback [3]–[7]. Linewidth narrowing and broadening [3], threshold change [4]–[6], mode-hopping, coherence collapse, and intensity-noise degradation [7] have been observed depending on the strength and phase of feedback. However, theoretical modeling of VCSEL's operating under feedback conditions has used numerical models which neglect spatial effects [8], [9]. Since VCSEL's have relatively large transverse dimensions, spatial effects such as spatial hole burning (SHB) and carrier diffusion are expected to be important, especially because VCSEL's often operate in several transverse modes at high injection currents [2]. It has been shown that VCSEL's exhibit static and dynamic characteristics significantly different from those of edge-emitting lasers because of SHB [10]–[12]. Such spatial effects are also expected to affect VCSEL operation under feedback conditions. Indeed, for short external cavities, a very recent study has shown that SHB can lead to the suppression of a higher order transverse mode under appropriate feedback conditions [13]. However, there has been little theoretical study on feedback-induced dynamics. It has been shown that edge-emitting lasers can follow both quasi-periodic and period-doubling routes to chaos as feedback is increased, under both single-mode and multimode conditions [14]. Whether VCSEL's show similar behaviors is an interesting issue that remains to be explored, both theoretically and experimentally.

In this paper, we investigate numerically the static and dynamic characteristics of VCSEL's under feedback conditions for single-mode and two-mode operations. We extend the study presented in [13] to include the cases of both short and long external cavities. Further, we consider two-mode operations with different transverse modes to assess the role of intermodal coupling induced by SHB. Our model, described in Section II, includes the spatial dependence of both the optical field and the carrier density. Section III discusses changes in the continuous-wave (CW) mode powers occurring with feedback for the case of short external cavities. It is found that even a relatively weak feedback such as reflection from a fiber tip (4% reflectivity) can turn two-mode operation into single-mode operation under appropriate conditions. Section IV studies the change in dynamics associated with feedback for long external cavities. Feedback from an external cavity as short as 1 cm can destabilize the CW operation, leading to period-doubling and chaos. The effects of SHB and different contact geometries are considered in each case.

II. Computer Model and Parameters

Assuming that the VCSEL can operate in two transverse modes simultaneously, the rate equations in the cylindrical coordinates are written as [10]

$$\frac{dE_i}{dt} = \frac{1}{2}\{(1-i\alpha)G_i(t) - \gamma_i\}E_i + \sum_{m=1}^{M} \kappa_m E_i(t-m\tau)e^{im\omega_i\tau} \tag{1}$$

$$\frac{\partial N}{\partial t} = D\nabla_T^2 N + \frac{J(r,\phi)}{qd} - \frac{N}{\tau_e} - BN^2 - \frac{1}{d}\sum_{i=1}^{2} G_{\text{local}}|E_i(t)|^2|\psi_i(r,\phi)|^2 \tag{2}$$

Manuscript received November 26, 1996; revised March 17, 1997. This work was supported in part by the U.S. Army Research Office and by the National Science Foundation under Grant PHY94-15583.

The authors are with the The Institute of Optics and Rochester Theory Center, University of Rochester, Rochester, NY 14627 USA.

Publisher Item Identifier S 1077-260X(97)04593-0.

where $E_i(t)$ is the amplitude of the ith transverse mode with the spatial distribution $\psi_i(r, \phi)$, $N(r, \phi, t)$ is the carrier density, α is the linewidth enhancement factor, and $G_i(t)$ and γ_i are the gain and cavity loss for the ith mode. In (2), τ_e is the carrier lifetime due to nonradiative recombination, D is the diffusion coefficient, B is the spontaneous recombination coefficient, d is the thickness of the active layer, and $J(r, \phi)$ is the injection current density. In the small-signal regime, the local gain $G_{\text{local}} = \sigma(N - N_T)$ is assumed to be linearly proportional to the local carrier density $N(r, \phi, t)$ and N_T is the carrier density at transparency. The modal gain $G_i(t)$ for each mode in (1) is obtained by calculating the spatial overlap between the local-gain profile and the spatial intensity distribution $|\psi_i(r, \phi)|^2$ of that mode.

Optical feedback through multiple round-trips is taken into account by the summation in the last term on the right-hand side of (1) [15]. κ_m is the feedback parameter for the the ith mode after m external-cavity round-trips each of duration τ, and M is the total number of round-trips included in the model. In general, cross coupling among different transverse modes should be included. However, cross coupling can be neglected for the two-mode case studied here since the two modes generally have orthogonal polarizations [2]. The parameter κ_m has a form similar to that for edge-emitting lasers [14] and is given by

$$\kappa_m = \frac{F_{\text{ext}} f^{m-1}}{\tau_L} \tag{3}$$

where the feedback parameter F_{ext} is defined as

$$F_{\text{ext}} = \frac{1 - R_2}{\sqrt{R_2}} \sqrt{R_{\text{ext}} \eta_c} \tag{4}$$

where R_2 and R_{ext} are the output-mirror and external-mirror reflectivities, τ_L is the solitary-laser round-trip time, and η_c is the coupling efficiency of the returned light to the optical field in the laser cavity. In general, η_c can be different for different modes. In this study, the feedback light is assumed to be a one-to-one image of the VCSEL aperture so that $\eta_c = 1$. Further, η_c is taken to be mode independent. The fraction f accounts for reduction in the feedback on successive round-trips in the external cavity and is given by

$$f = -\sqrt{R_2 R_{\text{ext}}}. \tag{5}$$

Because of high reflectivities of VCSEL mirrors ($R_2 >$ 99%), it is essential to include multiple round-trips in the external cavity even for $R_{\text{ext}} > 1\%$, in contrast with the case of edge-emitting lasers. The number of external-cavity round-trips M used in simulations is the smallest integer for which $\kappa_M/\kappa_1 < 0.1$. This approximation neglects feedback terms whose power is smaller than 1% of the dominant feedback term.

Equations (1) and (2) are solved numerically by using a finite-difference method with spatial and temporal resolutions of 0.1 μm and 0.1 ps, respectively. An index-guided VCSEL with cylindrical geometry (index guiding over 4-μm radius) is considered. The active region consists of three 8-nm quantum wells (QW's). Relevant device parameters are listed in Table I. Single-mode operation can be realized by using a disc contact of 2-μm radius such that current is injected only over a small central part of the VCSEL top area. The LP_{01} mode is then preferentially excited. For two-mode operation, different transverse modes can be excited by two different contact geometries. A 4-μm-radius disc contact excites the LP_{01} and LP_{11} modes, and a ring contact of inner and outer radii of 1.8 and 2.8 μm excites the LP_{11} and LP_{21} modes. These two cases will be referred to as the disc-contact and ring-contact geometries, respectively, in the following sections. The bias current is fixed at two times threshold throughout this study.

TABLE I
DEVICE PARAMETERS USED IN SIMULATIONS

Laser cavity length L_{eff}	2 μm
Solitary-laser round-trip time τ_L	0.045 ps
Active-region thickness (3 QWs)	3×8 nm
Radius of device	10 μm
Radius of index-guiding region	4 μm
Diffusion constant D	30 cm^2/s
Nonradiative recombination time τ_e	5 ns
Bimolecular recombination coefficient B	1×10^{-10} cm^3/s
Refractive indices n_1, n_2	3.4, 3.5
Wavelength λ	0.875 μm
Gain cross-section a_0	2.0×10^{-16} cm^2
Carrier density at transparency N_T	2.2×10^{18} cm^{-3}
Linewidth enhancement factor α	3
Mirror reflectivities R_1, R_2	0.995
Internal loss α_{int}	20 cm^{-1}
Longitudinal confinement factor Γ_l	0.012
Bias	$2 \times$ Threshold

III. SHORT EXTERNAL CAVITIES

In this section, we first focus on short external cavities. In practice, this corresponds to the case when a VCSEL is butt-coupled to an optical fiber, but there is a small air gap between the fiber and the VCSEL. We take R_{ext} to be 4%, the typical value of reflectivity from the tip of an optical fiber. Because of 99.5% reflectivity of VCSEL mirrors ($R_2 = 99.5\%$), (4) results in a relatively weak feedback ($F_{\text{ext}} \sim 10^{-3}$) even for $R_{\text{ext}} = 4\%$. Numerical simulations show that feedback does not destabilize the CW operation of VCSEL's for such short external cavities. However, feedback does affect the output powers considerably.

Fig. 1(a) shows the change of CW power with external-cavity length L_{ext} for single-mode (LP_{01}) operation by choosing $R_{\text{ext}} = 4\%$ and $\eta_c = 1$. Depending on the feedback phase, the returning field interferes constructively or destructively with the field in the laser cavity, resulting in a periodic change in power with external-cavity length on a wavelength scale. Feedback-induced power variations can exceed 20% of the CW power without feedback.

Results for two-mode operation excited by a disc contact are shown in Fig. 1(b). At two times above threshold, the output powers without feedback are 0.7 mW for both modes. Mode powers follow a periodic pattern similar to that of the single-mode case, but power variations of the two modes are neither in phase nor sinusoidal. Since the frequency difference between the LP_{01} and LP_{11} transverse modes ($\sim$150 GHz) corresponds to a negligibly small round-trip phase difference (about 0.03 radian), the phase shift observed in Fig. 1(b)

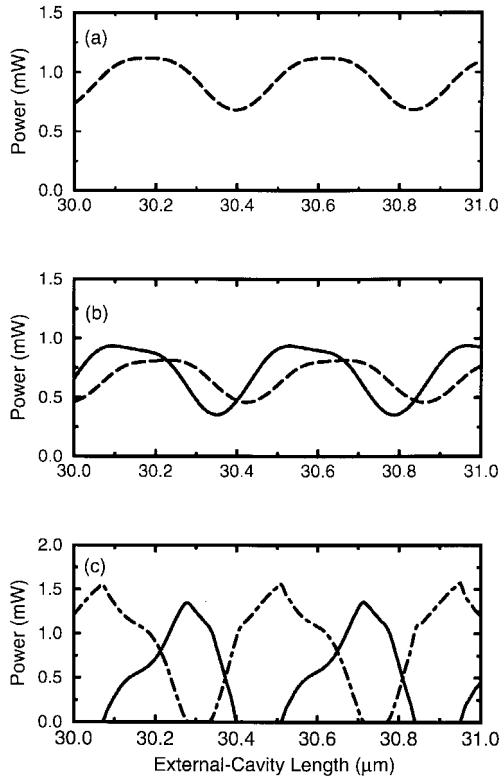

Fig. 1. Variations of mode power with external-cavity length. (a) Single-mode operation; two-mode operation excited by (b) disc-contact and (c) ring-contact geometry. Dashed, solid, and dot–dashed traces correspond to the LP_{01}, LP_{11}, and LP_{21} modes, respectively.

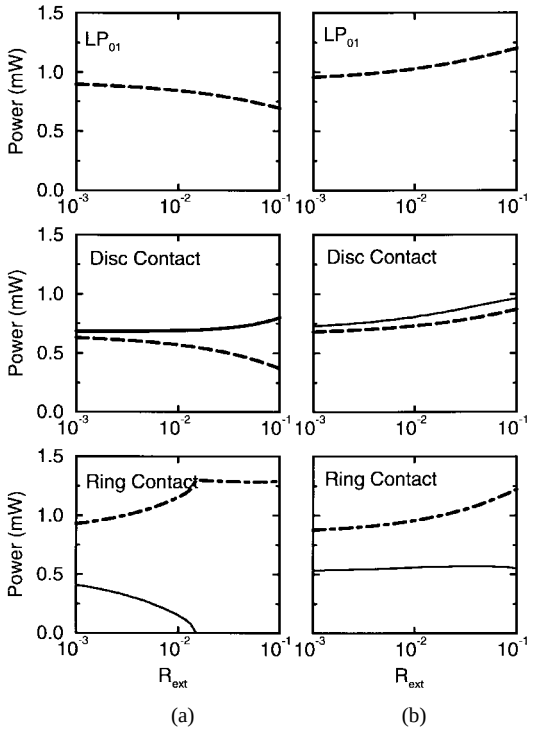

Fig. 2. Variations of mode power with external mirror reflectivity $R_{\rm ext}$ for two different external-cavity lengths. (a) $L_{\rm ext} = 30.45$ μm. (b) $L_{\rm ext} = 30.6$ μm. Dashed, solid, and dot–dashed traces correspond to the LP_{01}, LP_{11}, and LP_{21} modes, respectively.

cannot be attributed to it. Instead, the origin of the phase difference lies in mode coupling induced by SHB. When the power in the one mode is enhanced by feedback, the power in the other mode is slightly reduced due to SHB. Since the overlap between the spatial distributions of the LP_{01} and LP_{11} is relatively small, the effects of SHB are not very strong. Therefore, the magnitude of change in power is roughly the same as that for the single-mode case.

To study the strong mode-coupling case, calculations are repeated for the case of a ring contact, and results are shown in Fig. 1(c). Since the spatial distributions of the LP_{11} and LP_{21} overlap strongly, mode competition induced by SHB is severe. The enhancement of one mode leads to simultaneous suppression of the other mode to such an extent that the two modes are forced to be out of phase, and this behavior is relatively independent of the absolute value of the feedback phase. Strong mode-coupling also results in a larger change in mode powers compared with the case of single-mode operation [Fig. 1(a)]. In particular, one mode can be completely extinguished when the other mode has maximum power. This behavior can be useful in practice since it can be used to force operation in a single transverse mode even though the VCSEL normally operates in two transverse modes. By the same token, it suggests that the fiber tip position should remain fixed to a tolerance level below 0.1 μm if the objective is to avoid feedback-induced power variations.

To further investigate the effects of SHB, the mode powers are calculated for different values of the external reflectivities $R_{\rm ext}$ for two fixed external-cavity lengths, where η_c is chosen to be 1. Results for the two cases of $L_{\rm ext} = 30.45$ μm (left column) and 30.6 μm (right column) are plotted in Fig. 2, where $R_{\rm ext}$ is varied in the range 0.1%–10%. As expected, the magnitude of power variations increases with the amount of feedback. In the absence of mode coupling, both modes are expected to show an identical dependence on $R_{\rm ext}$ as given by the single-mode case (top row of Fig. 2) apart from a negligibly small phase difference. For two-mode operation, the direction as well as the magnitude of change in power are quite different from those of the single-mode case due to mode coupling induced by SHB. This difference is especially pronounced for large feedback values. In particular, for the case of a ring contact, powers in the two modes generally change in different directions as the feedback is increased because of increased mode competition induced by SHB. Complete turn-off of the LP_{11} mode occurs for $R_{\rm ext} \geq 3\%$ (lower left of Fig. 2).

IV. Long External Cavities

Since distant reflections can affect the dynamics of semiconductor lasers differently compared with near reflections [14], it is interesting to study the case where the external cavity is relatively long. In practice, this case corresponds to the configuration where the VCSEL light is focused onto a target by a lens. We choose $L_{\rm ext} = 1$ cm and investigate the change in VCSEL dynamics associated with the feedback strength $F_{\rm ext}$ by constructing the bifurcation diagram. For each value of $F_{\rm ext}$, after integrating the rate (1) and (2) over a temporal window of 10 ns to eliminate the transients, the maximum and

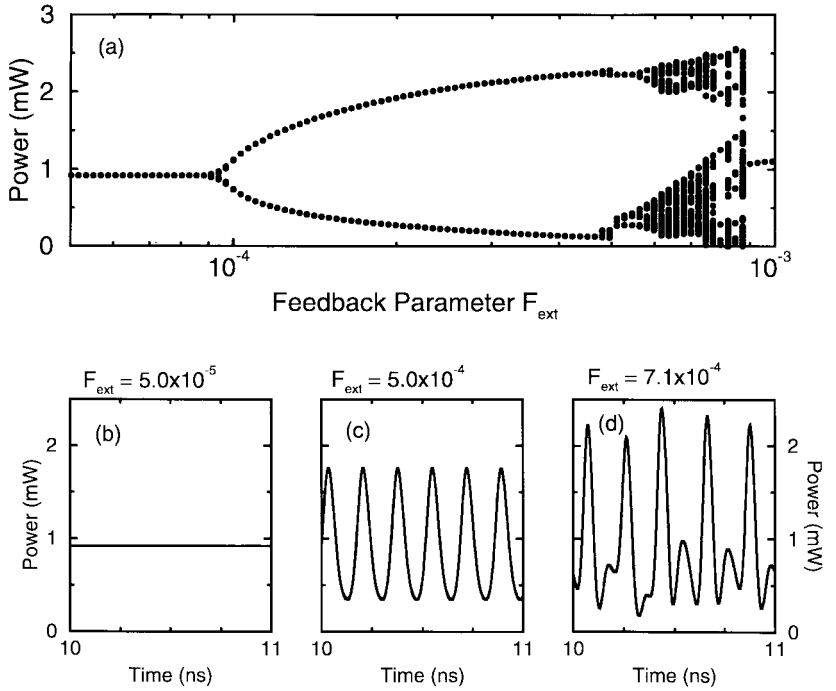

Fig. 3. (a) Bifurcation diagram with respect to the feedback parameter $F_{\rm ext}$ under single-mode operation for $L_{\rm ext} = 1$ cm. Temporal variations of mode power at three selected values of $F_{\rm ext}$ are shown as plots (b)–(d).

minimum powers in a subsequent 6-ns temporal window are sampled and plotted. The bifurcation diagram for single-mode (LP_{01}) operation along with three temporal traces at selected values of $F_{\rm ext}$ are shown in Fig. 3. A single point in the bifurcation diagram represents CW operation [Fig. 3(b)], two points represent period-one oscillations [Fig. 3(c)], and so on. As the feedback parameter is increased, the CW state becomes unstable due to undamping of relaxation oscillations, leading to self-pulsations at the relaxation-oscillation frequency [Fig. 3(b) and (c)] and subsequent chaotic behavior [Fig. 3(d)]. A similar behavior has been predicted for single-longitudinal-mode edge-emitting lasers [14].

We next consider the case of two-mode operation excited by a ring contact. The bifurcation diagram along with temporal traces for three chosen values of $F_{\rm ext}$ are shown in Fig. 4. Dots and solid lines represent the LP_{11} mode, and triangles and dashed lines represent the LP_{21} mode. At low feedback values, the two modes show stable CW operation. As feedback is increased, the two modes exhibit period-one oscillations followed by subsequent period-doubling, eventually leading to chaos. However, due to strong coupling between the two modes through SHB, self-pulsations and onset of chaos occur at much higher feedback values of $F_{\rm ext} > 4 \times 10^{-4}$, more than four times larger than that for single-mode operation. Similar delay of onset of chaos has been predicted for multilongitudinal-mode edge-emitting lasers [14]. Since all longitudinal modes of an edge-emitting laser have the same spatial distributions, it is understandable that they exhibit feedback dynamics similar to those of multiple-transverse-mode VCSEL's whose modal profiles overlap strongly.

Calculations are repeated for two-mode operation excited by a disc contact. Results are presented in Fig. 5. Dots and solid lines represent the LP_{01} mode, and triangles and dashed lines represent the LP_{11} mode. Due to partial overlap of the LP_{01} and LP_{11} modes, effects of SHB are weak compared with the previous case, resulting in quite different features. At low feedback levels, the two modes carry comparable amount of powers and behave like two independent distinct single modes [Fig. 5(b)]. Therefore, the onset of self-pulsations occurs at roughly the same value for the feedback parameter ($F_{ext} \sim 9 \times 10^{-5}$) as in the single-mode case. However, at moderate feedback levels ($F_{\rm ext} > 9 \times 10^{-5}$), mode-power enhancement due to feedback increases the strength of SHB, which results in period-doubling behavior and an earlier onset of chaos compared with the single-mode case.

Since the nonlinear dynamics is known to be affected significantly by the nonlinear gain [16], we have investigated its effect by varying the nonlinear-gain parameter $\epsilon_{\rm NL}$ in the range 0–5 $\times$ 10^{-17} cm^3. For $\epsilon_{\rm NL} < 1 \times 10^{-17}$ cm^3, the results presented here remain unchanged qualitatively. For larger values of $\epsilon_{\rm NL}$, the nonlinear dynamics seen in Figs. 3–5 are affected considerably by the nonlinear-gain effects.

V. Conclusion

We have investigated the effects of optical feedback on static and dynamic characteristics of VCSEL's, under both single-mode and two-mode operations. For short external cavities, mode power varies with the external cavity length on a wavelength scale due to constructive and destructive interference effects introduced by the feedback field. For single-mode operation, the direction of power change is completely determined by the feedback phase. However, for the two-mode case, optical feedback enhances the effects of SHB so that the magnitude and direction of power variations are significantly affected. In particular, for the case of two modes whose

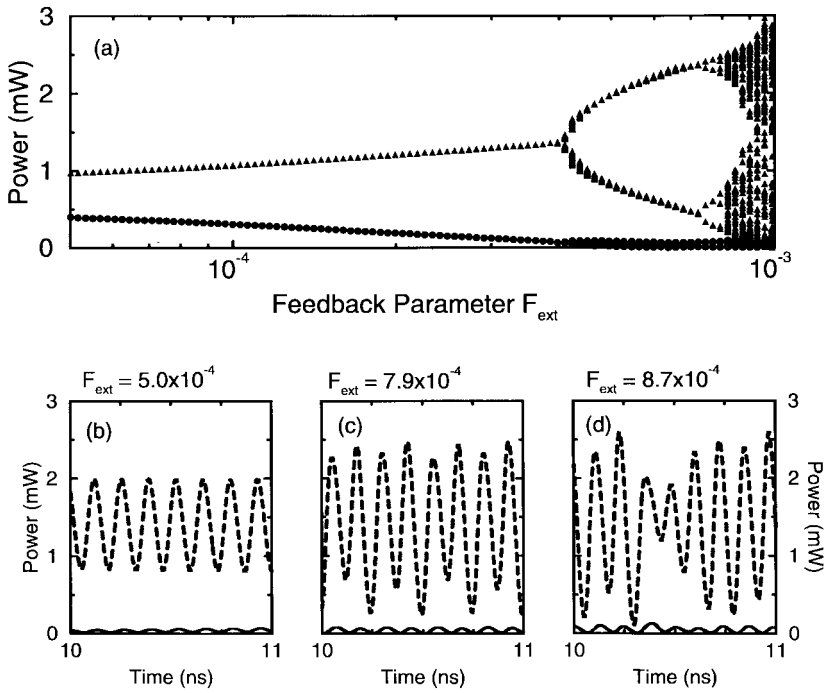

Fig. 4. (a) Bifurcation diagram with respect to the feedback parameter $F_{\rm ext}$ under two-mode operation excited by a ring contact for $L_{\rm ext} = 1$ cm. Temporal variations of mode powers at three selected values of $F_{\rm ext}$ are shown as plots (b)–(d). Dots and solid lines correspond to the $\rm LP_{11}$ mode, and triangles and dashed lines correspond to the $\rm LP_{21}$ mode.

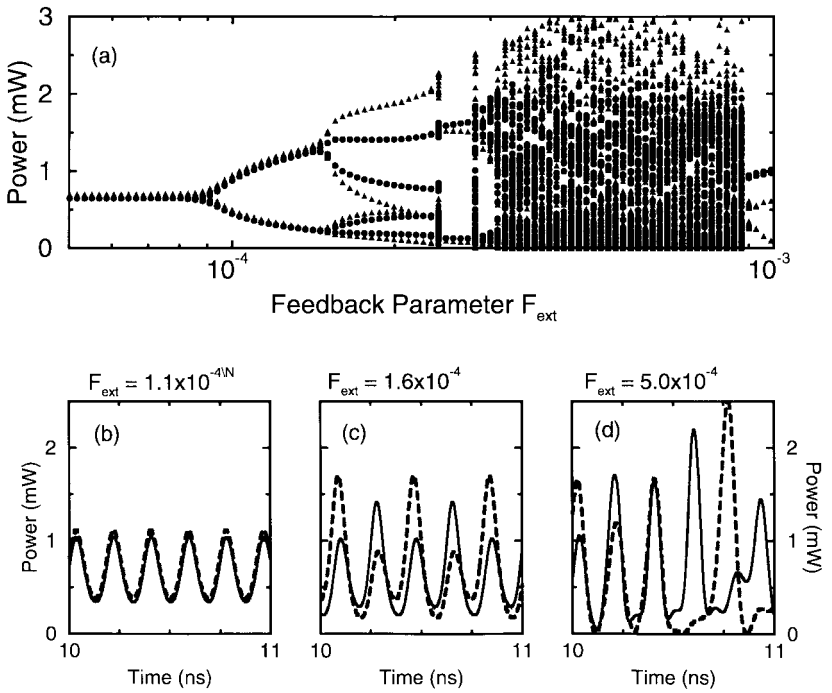

Fig. 5. (a) Bifurcation diagram with respect to the feedback parameter $F_{\rm ext}$ under two-mode operation excited by a disc contact for $L_{\rm ext} = 1$ cm. Temporal variations of mode powers at three selected values of $F_{\rm ext}$ are shown as plots (b)–(d). Dots and solid lines correspond to the $\rm LP_{01}$ mode, and triangles and dashed lines correspond to the $\rm LP_{11}$ mode.

intensity profiles overlap considerably, SHB forces power variations in different modes to be out of phase with respect to the external-cavity length. Furthermore, the magnitude of change in power can be so large that one transverse mode is completely suppressed.

For long external cavities, we have explored the change in dynamics associated with feedback. It is found that feedback dynamics for two-mode operation depends on the strength of mode competition induced by SHB. For the two modes whose spatial profiles overlap only partially, the two modes maintain some degree of independence, and relatively weak mode competition leads to period doubling and an earlier onset of chaos. In contrast, for the two modes whose spatial profiles overlap significantly, strong coupling between the two modes

results in reduced sensitivity toward feedback together with a delay in the onset of chaos.

REFERENCES

[1] C. J. Chang-Hasnain, *Semiconductor Lasers: Past, Present and Future*, G. P. Agrawal, Ed. Woodbury, NY: AIP Press, 1995, ch. 5.

[2] C. J. Chang-Hasnain, J. P. Harbison, G. Hasnain, A. C. Von Lehmen, L. T. Florez, and N. G. Stoffel, "Dynamic, polarization and transverse mode characteristics of VCSEL's," *IEEE J. Quantum Electron.*, vol. 27, pp. 1402–1408, 1991.

[3] Y. C. Chong and Y. H. Lee, "Spectral characteristics of VCSEL with external optical feedback," *IEEE Photon. Technol. Lett.*, vol. 3, pp. 597–599, 1991.

[4] U. Fiedler, "Design of VCSEL's for feedback insensitive data transmission and external cavity active mode-locking," *IEEE J. Select. Topics Quantum Electron.*, vol. 1, pp. 442–449, 1995.

[5] R. A. Morgan, G. D. Guth, M. W. Focht, M. T. Asom, K. Kojima, L. E. Rogers, and S. E. Callis, "Transverse mode control of vertical-cavity top-surface-emitting lasers," *IEEE Photon. Technol. Lett.*, vol. 4, pp. 374–377, 1993.

[6] G. C. Wilson, M. A. Hadley, J. S. Smith, and K. Y. Lau, "High single-mode output power from compact external microcavity surface-emitting laser diode," *Appl. Phys. Lett.*, vol. 63, pp. 3265–3267, 1993.

[7] K. P. Ho, J. D. Walker, and J. M. Kahn, "External optical feedback effects on intensity noise of vertical-cavity surface-emitting lasers," *IEEE J. Quantum Electron.*, vol. 29, pp. 892–895, 1993.

[8] H. M. Chen, K. Tai, K. F. Huang, Y. H. Kao, and J. D. Wynn, "Instability in SEL due to external optical feedback," *J. Appl. Phys.*, vol. 73, pp. 16–20, 1993.

[9] J. P. Zhang, "Numerical simulation For VCSEL with external optical feedback," *Microwave Opt. Tech. Lett.*, vol. 7, pp. 359–361, 1994.

[10] A. Valle, J. Sarma, and K. A. Shore, "Spatial hole-burning effects on the dynamics of vertical-cavity surface-emitting laser diodes," *IEEE J. Quantum Electron.*, vol. 31, pp. 1423–1431, 1995.

[11] G. C. Wilson, D. M. Kuchta, J. D. Walker, and J. S. Smith, "Spatial hole-burning and self-focusing in vertical-cavity surface-emitting laser diodes," *Appl. Phys. Lett.*, vol. 64, pp. 542–544, 1994.

[12] D. Vakhshoori, J. D. Wynn, and G. J. Zydzik, "Top-surface emitting lasers with 1.9V threshold voltage and the effect of spatial hole-burning on their transverse mode operation and efficiencies," *Appl. Phys. Lett.*, vol. 62, pp. 148–150, 1993.

[13] J. Dellunde, A. Valle, and K. A. Shore, "Transverse-mode selection in external-cavity vertical-cavity surface-emitting laser diodes," *J. Opt. Soc. Amer. B*, vol. 13, pp. 2477–2483, 1997.

[14] A. T. Ryan, G. P. Agrawal, G. R. Gray, and E. C. Cage, "Optical-feedback-induced chaos and its control in multimode semiconductor lasers," *IEEE J. Quantum Electron.*, vol. 30, pp. 668–679, 1994.

[15] R. Lang and K. Kobayashi, "External optical feedback effects on semiconductor injection laser properties," *IEEE J. Quantum Electron.*, vol. QE-16, pp. 327–355, 1980.

[16] G. P. Agrawal, "Effect of gain nonlinearities on period doubling and chaos in directly modulated semiconductor lasers," *Appl. Phys. Lett.*, vol. 49, pp. 1013–1015, 1986.

Joanne Y. Law received the B.S. degree in engineering from Brown University, Providence, RI, in 1993 and the M.S.E.E. degree from Stanford University, Stanford, CA, in 1994. She is currently pursuing the Ph.D. degree at the Institute of Optics, University of Rochester, Rochester, NY. Her dissertation work focuses on the multimode characteristics of vertical-cavity surface-emitting lasers with optical injection and feedback.

Govind P. Agrawal (M'83–SM'86–F'96) received the B.S. degree from the University of Lucknow in 1969 and the M.S. and Ph.D. degrees from the Indian Institute of Technology, New Delhi, in 1971 and 1974, respectively.

After holding positions at the Ecole Polytechnique, France, the City University of New York, New York, and AT&T Bell Laboratories, Murray Hill, NJ, he joined the faculty of the Institute of Optics at the University of Rochester, Rochester, NY, in 1989, where he is a Professor of Optics. His research interests focus on quantum electronics, nonlinear optics, and laser physics. In particular, he has contributed significantly to the fields of semiconductor lasers, nonlinear fiber optics, and optical communications. He is an author or co-author of more than 200 research papers, several book chapters and review articles, and three books entitled *Fiber-Optic Communication Systems* (New York: Wiley, 1992), *Semiconductor Lasers* (New York: Van Nostrand Reinhold, 1993), and *Nonlinear Fiber Optics* (New York: Academic, 1995). He has also edited the books *Contemporary Nonlinear Optics* (New York: Academic, 1992) and *Semiconductor Lasers: Past, Present and Future* (Woodbury, NY: AIP Press, 1995).

Dr. Agrawal is a fellow of the Optical Society of America.